Journal of Inorganic Biochemistry 273 (2025) 113026

Contents lists available at ScienceDirect

Journal of Inorganic Biochemistry

journal homepage: www.elsevier.com/locate/jinorgbio

Engineered hemoproteins containing non-canonical cofactors toward artificial metalloenzymes

Koji Oohora [a,b,*]

[a] Department of Applied Chemistry, Graduate School of Engineering, The University of Osaka, Suita, Osaka 565-0871, Japan
[b] Innovative Catalysis Science Division, Institute for Open and Transdisciplinary Research Initiatives (ICS-OTRI), The University of Osaka, Suita, Osaka 565-0871, Japan

ARTICLE INFO

Keywords:
Artificial metalloenzyme
Heme
Pophryrinoid
Catalysis

ABSTRACT

Hemoproteins have emerged as versatile scaffolds for the construction of artificial metalloenzymes. Through directed evolution via random and/or site-saturation mutagenesis, these proteins can be repurposed to catalyze abiological transformations. Their catalytic scope can be further expanded by introducing non-canonical molecular components. One approach involves the incorporation of non-canonical amino acid residues, such as methylhistidine, into the protein scaffold. Another strategy replaces the native heme with synthetic cofactors. While natural heme cofactors are generally restricted to porphyrins, synthetic chemistry has enabled access to a variety of porphyrin derivatives and artificial porphyrinoids with diverse core structures and peripheral functionalities. This review highlights recent efforts in designing such non-canonical cofactors and engineering complementary protein mutants to achieve challenging transformations, including C–H hydroxylation/amination and olefin cyclopropanation. Expanding the chemical space of hemoproteins through the integration of non-canonical cofactors represents a promising direction toward artificial metalloenzymes with novel and valuable catalytic functions.

1. Introduction

Metalloenzymes, enzymes that contain metal ions or metal cofactors as active centers, are responsible for approximately 30 % of all known enzymatic reactions in biological systems [1]. These enzymes facilitate a wide range of chemical transformations, including some of the most challenging ones such as C–H functionalization, methyl group transfer, and nitrogen fixation, all under mild physiological conditions [2]. Despite the limited availability of metal ions and ligands in nature, living systems have evolved highly effective metalloenzymes through the integration of metal cofactors with finely tuned protein matrices. These protein scaffolds not only provide a structural framework for the metal center but also play a crucial role in regulating its reactivity. In natural systems, metalloenzymes exhibit exceptional catalytic properties by coordinating the metal center with specific amino acid residues such as histidine, cysteine, methionine, aspartate, glutamate, tyrosine, and serine. These ligating residues contribute to the fine-tuning of the electronic properties and redox potential of the metal center. Beyond direct ligation, the protein scaffold creates a highly organized second coordination sphere composed of non-covalent interactions such as hydrogen bonding, electrostatic, and hydrophobic interactions [3]. These interactions assist in substrate positioning, proton and electron transfer, and transition-state stabilization, collectively orchestrating complex reaction pathways with high selectivity and efficiency. Among various classes of metalloenzymes, hemoproteins have received significant attention due to their structural simplicity, versatility, and catalytic potential. Hemoproteins contain heme, an iron-porphyrin complex, as their central cofactor. The most common natural form, heme *b* (iron protoporphyrin IX), is typically non-covalently bound within a hydrophobic pocket of the protein (Fig. 1a) [4,5]. Despite the uniformity of the heme cofactor, hemoproteins serve diverse biological functions such as oxygen transport and storage (e.g., myoglobin), redox reactions (e.g., cytochromes), and oxidative catalysis (e.g., cytochrome P450s). Myoglobin (Mb), one of the earliest structurally characterized proteins, contains a heme *b* cofactor embedded within an α-helical globular protein matrix [6]. The iron center is ligated by a proximal histidine residue, while a distal histidine provides hydrogen bonding that stabilizes bound dioxygen. Substitution of the distal histidine with non-polar residues drastically reduces oxygen affinity, illustrating the sensitivity of hemoprotein function to second-sphere interactions. This interplay between metal cofactor and protein environment exemplifies the modular nature of hemoproteins and provides a platform for

* Corresponding author at: Department of Applied Chemistry, Graduate School of Engineering, The University of Osaka, Suita, Osaka 565-0871, Japan.
E-mail address: oohora@chem.eng.osaka-u.ac.jp.

https://doi.org/10.1016/j.jinorgbio.2025.113026
Received 30 April 2025; Received in revised form 28 July 2025; Accepted 7 August 2025
Available online 9 August 2025

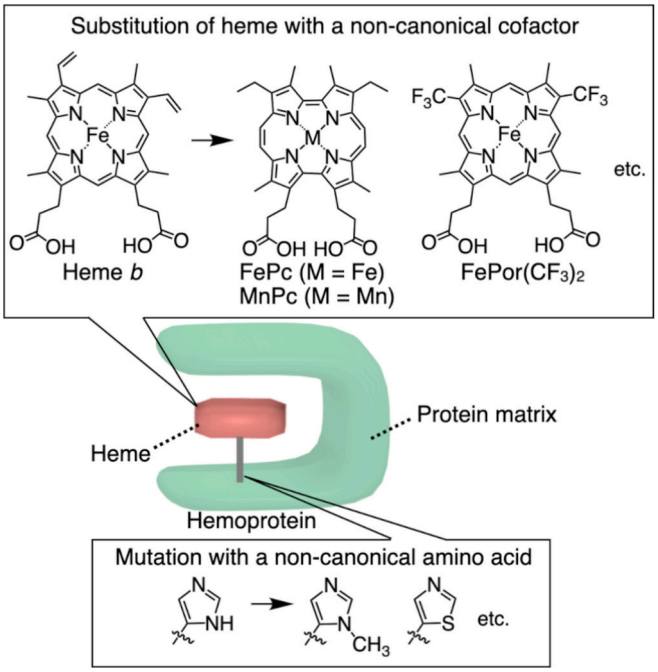

Fig. 1. Schematic representation for engineering of hemoprotein by non-canonical molecular components.

engineering new functions.

Cytochrome P450 enzymes, another well-studied class of hemoproteins, utilize a thiolate-ligated heme cofactor to catalyze a range of oxidative transformations, including C–H hydroxylation, epoxidation, and heteroatom oxidation [4]. These reactions proceed through high-valent iron-oxo intermediates, often referred to as compound I, which are generated via dioxygen activation in the presence of electron donors. Importantly, the redox potential and spin state of the heme iron can be modulated by the surrounding protein environment, including hydrogen bonding to the axial cysteine and neighboring residues. This demonstrates how subtle changes in the protein matrix can dramatically influence reactivity. The capacity of hemoproteins to stabilize reactive intermediates and support diverse transformations under mild conditions has inspired efforts to redesign them as artificial metalloenzymes. Protein engineering techniques, including site-directed mutagenesis and directed evolution, have enabled the repurposing of natural hemoproteins toward new-to-nature catalysis [7–20]. These engineered enzymes can perform reactions unknown in biology, such as carbene and nitrene transfer, through the formation of synthetic metal intermediates. In this context, hemoproteins are particularly well-suited for customization because their metal cofactor is removable and replaceable, and their active sites are tolerant of mutations. The combination of a well-defined metal center and a flexible protein scaffold enables precise tuning of reactivity. These features make hemoproteins attractive candidates for the development of artificial metalloenzymes with broad substrate scope, improved activity, and enhanced selectivity. This growing body of work demonstrates how hemoproteins can bridge the gap between synthetic coordination chemistry and enzymology. Their modular nature allows for systematic modification of both the primary and secondary coordination environments, unlocking access to non-natural reactivity. By harnessing their intrinsic properties and introducing rational modifications, hemoproteins have become powerful platforms for the creation of novel biocatalysts aimed at challenging synthetic transformations.

Expanding the chemical functionality of hemoproteins through non-canonical modifications has emerged as a promising approach for creating artificial metalloenzymes. As shown in Fig. 1b, two complementary strategies have received particular attention: the incorporation of non-canonical amino acid residues [21] and the substitution of native heme cofactors with synthetic metalloporphyrinoids [22,23]. These modifications, often carried out independently but increasingly explored in combination, allow precise tuning of the primary and secondary coordination environments and enable reactivity beyond the scope of natural systems. Incorporation of non-canonical amino acids into hemoproteins offers a powerful tool to modulate the coordination chemistry and electronic structure of the metal center. For example, Hilvert and coworkers engineered Mb variants containing N_δ-methyl histidine as a proximal ligand [24,25]. This modification enhanced both the peroxidase activity and cyclopropanation reactivity of Mb and enabled the crystallographic detection of a carbene intermediate—providing direct structural evidence of non-natural catalysis. Building on this, analogues such as 5-thiazoylalanine, 4-thiazoylalanine, and 3-(3-thienyl)alanine have been incorporated to probe their effects on carbene transfer [26]. Notably, Mb reconstituted with 4-thiazoylalanine exhibited superior activity for S–H bond insertion reactions, highlighting how subtle changes to the ligand sphere can modulate selectivity and efficiency. Axial ligand substitution is not limited to histidine analogues. For instance, Green and coworkers demonstrated that replacing the axial cysteine residue in CYP119 with selenocysteine improves catalytic activity for C–H bond hydroxylation [27]. This effect arises from altered redox properties and electron-donating ability of selenium versus sulfur, offering an elegant means to fine-tune oxidative power. Meanwhile, Lu and colleagues have constructed entirely new metal-binding environments in Mb by engineering distal histidine pockets that support copper binding, successfully mimicking the reactivity of enzymes such as nitric oxide reductase and cytochrome *c* oxidase. Genetic incorporation of imidazole-tethered tyrosine residues has also been shown to enhance dioxygen reduction activity [28].

Parallel to these protein engineering efforts, synthetic coordination chemistry has provided a broad range of artificial metal cofactors that can be introduced into hemoproteins. Reconstitution of hemoprotein enables the replacement of heme with designed metalloporphyrinoids bearing non-natural metals, ligands, or frameworks [22,23]. This modular approach has yielded artificial metalloenzymes with entirely new reactivities as summarized in Table 1. Significant examples include iridium-substituted Mb and CYP119, which catalyze a series of abiological reactions [29–33]. The incorporation of Ir-porphyrin into cytochrome P450 scaffolds has enabled the development of artificial metalloenzymes with unprecedented reactivity and selectivity. These engineered proteins catalyze a range of abiological carbene and nitrene transfer reactions, including cyclopropanation of internal and terminal alkenes, intramolecular C–H amination, and site-selective C–H alkylation via carbene insertion. Directed evolution of CYP119 variants has afforded enzymes with enhanced chemoselectivity, enabling transformations not achievable with native Fe-based hemoproteins. These Ir-substituted hemoproteins operate under mild, aqueous conditions, maintain robust protein scaffolds, and tolerate a wide substrate scope including medicinally relevant scaffolds. Importantly, Ir center modulates carbene reactivity, favoring productive insertion over unproductive side reactions. Together, these findings highlight the potential of Ir-substituted hemoproteins as versatile platforms for engineering new-to-nature enzymatic reactivities. Mn, Co, Ru and Rh porphyrins have also expanded the catalytic landscape of hemoproteins [34–39]. Mb reconstituted with Ru-porphyrin has emerged as a robust artificial metalloenzyme for promoting carbene transfer reactions. Lehnert and his coworkers demonstrated that Ru-substituted Mb catalyzes efficient cyclopropanation of olefins with ethyl diazoacetate (EDA) in aqueous buffer under mild conditions. Notably, the Ru center enables a catalytic pathway distinct from the native Fe heme, offering enhanced reactivity and stability. The enzyme retained its tertiary structure upon reconstitution, and the Ru–carbene intermediate might show improved reactivity, whereas unfavorable protein modification and degradation is competitive. Additionally, Fasan and coworkers reported that Ru- and Rh-substituted Mbs broaden the reaction scope to include C–H

Table 1
Representative catalysis by reconstituted hemoproteins with synthetic cofactors.

Protein Scaffold	Cofactor	Reaction	Substrate	Reagent	Catalytic Performance	Ref.
CYP119 mutants/ Mb mutants	Ir porphyrin	Cyclopropanation	Terminal and internal alkenes	EDA	Up to TON = 1300, 99 % ee	[29,31]
CYP119 mutants	Ir porphyrin	Intramolecular/ intermolecular C–H alkylation	Methoxybenzene derivatives/phthalan	-/EDA	Up to TON = 35,129, 98 % ee	[30,31]
Mb mutants	Ru porphyrin	Cyclopropanation	Styrene derivatives	EDA	Up to TON = 360, 96 % diastereoselectivity	[34]
Mb mutants /Cytochrome b_{562}/Heme oxygenase	Co porphyrin	CO_2 reduction	CO_2	$Ru(bipyridine)_3$ + ascorbic acid	Up to TON = 2000, 78 % CO selectivity	[39,36,37]
Mb mutants	$FePor(CF_3)_2$ /FePc	Cyclopropanation	Styrene	EDA	Up to TON = 810, 99 % ee	[41,47]
Mb mutants	FePc	Intramolecular C–H amination	Alkylbenzenesulfonyl azide	–	TON = 5.7×10^4, 96 % chemoselectivity	[48]
Mb mutants	MnPc	C–H hydroxylation	Ethylbenzene	$H_2O_2/H_2 + O_2$ + PdAu particles	Up to TON = 21, 69 % ee	[49,51,52]

alkylation via carbene insertion similar to Ir-substituted Mb. A Co-porphyrin complex introduced into hemoproteins has enabled photo-induced hydrogen evolution and CO_2 reduction that are inaccessible to the native protein. Ghirlanda's group demonstrated that Co-substituted cytochrome b_{562} variants exhibit light-driven CO_2 reduction activity, enabled by the incorporation of Co-porphyrin into the heme pocket. Lu and coworkers further expanded this concept by introducing Co-porphyrin cofactors into modified globin scaffolds, achieving selective CO_2-to-CO photoreduction under aqueous conditions. These studies highlight the feasibility of developing hemoprotein-based photocatalysts for sustainable energy applications using metal substitution strategies. Taken together, these examples illustrate that substitution of the iron center in heme with non-native transition metals can unlock diverse catalytic reactivities in hemoproteins. This strategy not only enables access to novel abiological transformations such as carbene and nitrene transfer, but also offers a route to designing artificial metalloenzymes for small-molecule activation, redox transformations, and photocatalytic processes.

Our group has systematically explored porphycene-based cofactors, finding that reconstituted Mb with Fe-porphycene exhibits elevated peroxidase and cyclopropanation activity, including the detection of catalytic intermediates by spectroscopic methods [40,41]. In some cases, the rate enhancement over native Mb was more than 25-fold. Other types of cofactors such as tetradehydrocorrins have proven valuable [42–45]. For example, reconstituted Mb with Ni-tetradehydrocorrin has mimicked the activity of methyl-coenzyme M reductase, including stabilization of a Ni(I) intermediate. These findings highlight how porphyrin framework modification, in addition to metal substitution, can dramatically alter the physicochemical properties and catalytic capabilities of hemoproteins. Importantly, these strategies are not mutually exclusive. Fasan's group demonstrated a system in which Mb was reconstituted with an iron complex of electron-deficient porphyrin (2,4-diacetyldeuteroporphyrin IX) while simultaneously incorporating a non-canonical N_δ-methyl histidine ligand [46]. This dual modification significantly improved cyclopropanation activity and enantioselectivity, offering a blueprint for future enzyme design. Therefore, the integration of non-canonical amino acids and artificial metal cofactors into hemoproteins provides a versatile and effective route to expanding enzymatic function. These modifications, which can be individually tailored or combined, offer unprecedented control over catalytic reactivity, selectivity, and substrate scope.

In this review, our recent works related to reconstituted hemoproteins with non-canonical cofactors are summarized: redox-tuning of reconstituted Mb toward enhanced cyclopropanation activity, C–H bond amination accelerated by Fe porphycene in Mb matrix, hybrid catalysis system containing reconstituted Mb and heterogeneous catalysts and rational design of reconstituted Mb mutants toward enantioselective C–H hydroxylation [47–50].

2. Redox tuning of reconstituted myoglobin for enhanced cyclopropanation

Olefin cyclopropanation via metal-carbenoid intermediates has become a representative reaction in artificial hemoprotein catalysis. While native Mb (nMb) and cytochrome P450 variants can generally catalyze the cyclopropanation of styrenes with diazo compounds, their activity toward more inert olefins remains limited. One key strategy to overcome this limitation involves tuning the redox potential of the iron center within the heme cofactor. Engineering a more positive redox potential can increase the electrophilicity of the carbene intermediate, thereby enhancing reactivity toward unactivated olefins. In this context, we investigated an iron porphyrin cofactor with two electron-withdrawing trifluoromethyl groups, $FePor(CF_3)_2$, and inserted it into apoMb (Fig. 1b). The resulting protein, rMb($FePor(CF_3)_2$), exhibited a redox potential of +147 mV vs NHE—significantly higher than nMb or Mb reconstituted with Fe-porphycene (rMb(FePc)). Crystal structure analysis confirmed that $FePor(CF_3)_2$ binds within the heme pocket without disturbing the overall protein architecture (Fig. 2). These findings illustrate that electronic modification of the cofactor is a powerful tool for modulating protein-bound redox chemistry without compromising structural integrity. The rMb($FePor(CF_3)_2$) catalyst showed greatly enhanced performance in styrene cyclopropanation reactions. When compared to nMb and rMb(FePc), rMb($FePor(CF_3)_2$) provided a highest turnover number (TON) of 710 and excellent diastereo- and enantioselectivity when paired with the engineered variant (H64V/V68A). Substitution patterns in styrene derivatives further confirmed that electron-deficient olefins benefited most from the increased redox potential. Notably, rMb($FePor(CF_3)_2$) displayed a five-fold increase in TON under limiting EDA concentrations compared to the cofactor alone. The positive effect of $FePor(CF_3)_2$ extended to internal

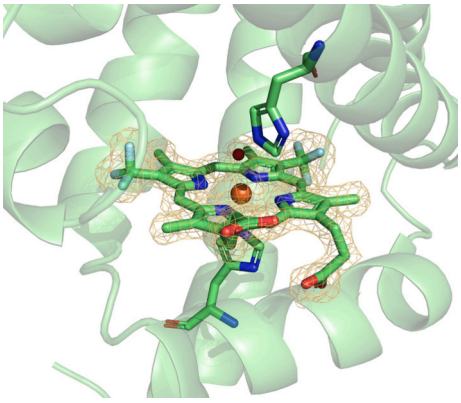

Fig. 2. Crystal structure of rMb($FePor(CF_3)_2$) (PDB ID: 8WF5).

and aliphatic olefins such as β-methylstyrene and 1-octene, where rMb ($FePor(CF_3)_2$) outperformed nMb with up to 165-fold higher TONs (Fig. 3). This result is particularly important because internal and aliphatic olefins are typically resistant to iron porphyrin-catalyzed cyclopropanation. By increasing the redox potential, we successfully accessed these previously unreactive substrates. One notable feature of rMb($FePor(CF_3)_2$) is its partial tolerance to molecular oxygen. Under aerobic conditions, and without added reductants, the catalyst retained a significant fraction of its activity. This contrasts with the total inactivity of nMb under similar conditions. The effect was especially pronounced when using the H64V/V68A mutant, which has reduced oxygen-binding affinity due to the removal of the distal His64 residue. The combination of a reactive electron-deficient cofactor and a low-oxygen-affinity scaffold enabled productive catalysis even in air. This aerobic performance expands the operational scope of artificial metalloenzymes and highlights the synergy between cofactor design and protein engineering. The ability to avoid sacrificial reductants in abiological reactions represents a significant step forward for green and scalable biocatalysis. Hammett studies revealed distinct mechanistic differences between rMb($FePor(CF_3)_2$), nMb, and rMb(FePc). The electron-deficient $FePor(CF_3)_2$ system showed high correlation with spin-delocalization parameters, suggesting a radical-type mechanism, while FePc followed a polar (electrophilic) pathway. Dual-parameter regression analysis confirmed this distinction, indicating divergent electronic structures of the respective carbene intermediates. Transient absorption spectroscopy failed to detect the short-lived active carbene species in rMb($FePor(CF_3)_2$), likely due to rapid transformation into unreactive adducts. Nevertheless, evidence from product distributions and Hammett plots supports a stepwise radical cyclopropanation pathway. Building on the radical character of the carbene species, we also explored C–H bond alkylation. Although the TON was modest (TON = 2), rMb($FePor(CF_3)_2$) catalyzed insertion into weak benzylic C–H bonds, representing a rare example of such activity using an iron-porphyrin system. This underscores the potential of redox-tuned artificial cofactors for expanding the reactivity of hemoproteins into new domains. Thus, the combination of protein engineering and cofactor substitution provides a robust strategy for enhancing the reactivity, selectivity, and versatility of artificial metalloenzymes. The investigation of rMb($FePor(CF_3)_2$) illustrates how fine-tuning redox potential can impact not only reaction efficiency but also mechanistic pathways and operational conditions.

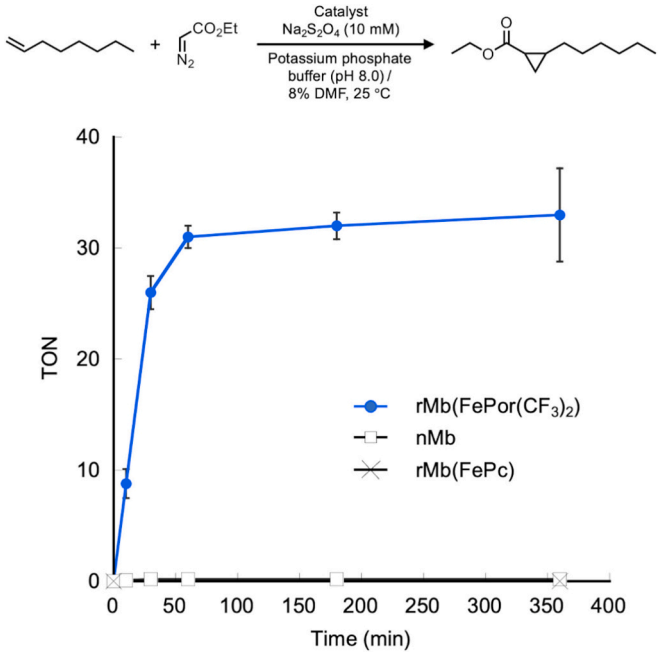

Fig. 3. Time course of TON for the catalytic cyclopropanation of 1-octene.

3. Intramolecular C–H bond amination catalyzed by myoglobin reconstituted with iron porphycene

The formation of carbon–nitrogen (C–N) bonds through direct C–H bond functionalization is a compelling approach in organic synthesis, providing efficient routes to nitrogen-containing compounds without pre-activation steps. Among the strategies developed, intramolecular C–H bond amination via nitrene transfer has attracted particular attention due to its atom economy and potential for site-selectivity. Transition metal catalysts, including metalloporphyrins, have proven effective in mediating these reactions. Inspired by the role of high-valent iron-oxo species in cytochrome P450 enzymes, synthetic analogs of metalloporphyrins have been developed to catalyze C–H bond amination through iron-nitrene intermediates. Here, rMb(FePc) was investigated for intramolecular C–H bond amination of arylsulfonyl azides (Fig. 1b). The unique electronic properties of porphycene offer altered redox potentials and the potential stabilization of reactive intermediates. rMb(FePc) exhibited remarkable catalytic activity and selectivity, outperforming nMb and FePc alone. In the reaction of 2,4,6-triisopropylbenzenesulfonyl azide, rMb(FePc) achieved a TON of 318 and a chemoselectivity of 96 %, far exceeding the performance of nMb (TON = 255, 80 % selectivity) and FePc alone (TON = 256, 78 % selectivity) (Table 2). The hydrophobic environment of the protein matrix appears to promote C–H bond amination while suppressing the undesired reduction of the nitrene intermediate to sulfonamide. Notably, when the catalyst loading was decreased to 0.001 mol%, the TON reached 5.7×10^4, the highest reported value for a biocatalytic tertiary C–H bond amination. Further evaluation with secondary benzylic C–H bonds using 2,4,6-triethylbenzenesulfonyl azide revealed lower TONs (7 for rMb(FePc)), attributed to stronger C–H bond dissociation energies. However, recombinant sperm whale myoglobin (rswMb) reconstituted with FePc showed improved activity (TON = 14) and chemoselectivity (4 %). To enhance enantioselectivity, His64 was mutated to alanine, valine, or isoleucine. Among these mutants, rswMbH64A(FePc) achieved the highest TON (25) and 27 % ee, while rswMbH64I(FePc) showed the highest enantioselectivity (37 % ee), highlighting the role of the distal residue in shaping chiral environments. Mechanistic studies provided insight into the reaction pathway. A linear correlation between the $\log(k_{obs})$ and C–H bond dissociation energy (BDE) across tertiary, secondary, and primary substrates indicated that hydrogen atom abstraction is a key step. The proposed mechanism involves reduction of FePc to its ferrous state, nitrene formation via azide activation, hydrogen abstraction from the substrate, and radical recombination to yield the product. Competing pathways involve proton-coupled reduction of the nitrene to sulfonamide. Kinetic analysis revealed that rMb(FePc) significantly enhances the catalytic

Table 2
TON values for catalytic C–H bond amination of 2,4,6-triisopropylbenzenesulfonyl azide.[a]

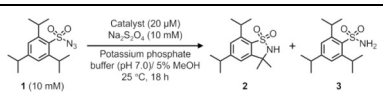

Entry	Catalyst	Yield (2)	TON (2)	2: 3
1	rMb(FePc)	64 %	318	96:4
2	nMb	51 %	255	80:20
3	FePc	51 %	256	78:22
4[b]	rMb(FePc)	57 %	5.7×10^4	85:15

[a] Conditions: [catalyst] = 20 μM, [$Na_2S_2O_4$] = 10 mM, [substrate] = 10 mM in 100 mM potassium phosphate buffer (pH 7.0) containing 5 % MeOH at 25 °C for 18 h under N_2 atmosphere. [b] [catalyst] = 0.1 μM.

turnover frequency (k_{cat} = 55 s^{-1}) compared to nMb (k_{cat} = 14 s^{-1}), while maintaining similar substrate affinity ($K_m \approx 1$ mM) (Fig. 4). This results in a nearly five-fold increase in catalytic efficiency relative to nMb (k_{cat}/K_m = 59 vs. 12 mM^{-1} s^{-1}). These improvements are likely due to facilitated nitrene formation or faster hydrogen abstraction enabled by the modified cofactor. Importantly, rMb(FePc) also exhibited slower rates in the undesired azide reduction pathway compared to nMb. This suggests that FePc substitution reduces the tendency of the metal-nitrene species to undergo two-electron reduction. The negatively shifted Fe(III)/Fe(II) redox potential of FePc (by over 200 mV) may be responsible for this behavior, helping to stabilize the nitrene intermediate and favor productive C–H bond insertion. The H64A mutation further decreased azide reduction, likely by removing a proton donor residue involved in facilitating nitrene reduction. Such an effect parallels prior studies in engineered cytochrome P450s, where proton relay residues were shown to modulate the competition between nitrene insertion and reduction pathways. Thus, the integration of iron porphycene as a synthetic cofactor and targeted mutation of distal residues in Mb enables efficient and selective intramolecular C–H bond amination. These findings not only expand the catalytic repertoire of artificial metalloenzymes but also offer mechanistic insights into the control of nitrene transfer reactivity. The strategy outlined here provides a design strategy for future development of enzyme catalysts for abiological transformations involving nitrogen-group transfer.

4. Hybrid catalysis for ethylbenzene oxidation using dioxygen

The selective oxidation of unactivated C(sp^3)–H bonds using dioxygen as a terminal oxidant is a central challenge in green chemistry. Cytochrome P450 enzymes accomplish such transformations in nature using a sophisticated network of redox proteins and cofactors, but these systems require NAD(*P*)H as sacrificial reductants and exhibit limited substrate scope. Inspired by the redox machinery of P450s, the development of hybrid catalytic systems that merge biocatalysts with inorganic catalysts offers a promising strategy for activating dioxygen without relying on expensive reductants. In this context, a hybrid catalysis system was developed combining a reconstituted myoglobin containing a manganese porphycene cofactor (rMb(MnPc)) with palladium-gold alloy nanoparticles (PdAu NPs) encapsulated in hollow mesoporous silica spheres ($Pd_1Au_{0.5}$@HMSS) (Fig. 5). While rMb(MnPc) alone can promote hydroxylation of ethylbenzene using H_2O_2, which was previously reported via a detectable Mn(V) = O species by our group [51,52], it cannot activate O_2 directly. PdAu NPs, on the other hand, catalyze the in situ production of H_2O_2 from H_2 and O_2 [53]. This system enables tandem catalysis: the PdAu NPs generate H_2O_2, which is then used by rMb(MnPc) to oxidize the substrate. The $Pd_1Au_{0.5}$@HMSS nanoparticles were optimized for H_2O_2 production. Under mixed H_2/O_2 atmosphere (0.5 atm each), H_2O_2 generation reached 0.4 mM at pH 8.5 with 5 mg/mL catalyst. Interestingly, NaCl significantly enhanced H_2O_2 accumulation: at 10 mM NaCl, H_2O_2 concentration increased to 0.6 mM. Higher catalyst concentrations did not lead to more H_2O_2, likely due to concurrent decomposition. These observations underscore the need for fine-tuning catalyst concentration and reaction conditions to maximize H_2O_2 availability without overaccumulation and subsequent degradation. The dependence of rMb(MnPc) activity on H_2O_2 concentration was carefully examined. Using externally added H_2O_2, hydroxylation of ethylbenzene showed a clear optimum at 10 mM (TON = 13). Lower concentrations led to reduced activity (TON = 4.4 at 0.5 mM), while excess H_2O_2 decreased efficiency, likely due to oxidative degradation of the porphycene cofactor. These findings reveal that H_2O_2 must be supplied in a controlled and sustained manner—a challenge effectively addressed by hybrid catalysis. Hybrid catalysis reactions were conducted by combining rMb(MnPc) with $Pd_1Au_{0.5}$@HMSS under a mixed atmosphere of H_2 and O_2. The system achieved ethylbenzene oxidation with a TON of 3.6 under optimized conditions (pH 8.5, 10 mM NaCl), which closely mirrors the TON observed using 0.5 mM exogenous H_2O_2. Importantly, control experiments confirmed that neither rMb(MnPc) nor PdAu NPs alone could accomplish this transformation under the same conditions. Additionally, the formation of acetophenone—a byproduct of overoxidation—was only observed in the presence of PdAu NPs, suggesting that the two catalysts operate independently without significant interference. NaCl had a dual effect: enhancing H_2O_2 generation and improving rMb(MnPc) activity. For example, at 10 mM NaCl, rMb(MnPc) activity increased from a TON of 5.1 to 7.1 using 1 mM H_2O_2. This additive effect likely arises from ionic strength modulation or stabilization of reactive intermediates. Gas-phase studies revealed that rMb(MnPc) activity was slightly affected by O_2 and H_2 concentrations but remained robust, indicating that the protein structure and activity were preserved in the hybrid system. The protective silica shell surrounding the PdAu NPs likely prevented protein deactivation by metal surfaces or reactive oxygen species. Overall, the hybrid system represents a modular and biomimetic strategy for alkyl C–H oxidation. By decoupling dioxygen activation from substrate oxidation, it overcomes limitations of natural redox partners and sacrificial electron donors. This approach highlights the synergy between artificial metalloenzymes and inorganic catalysts and opens avenues for integrating nanomaterials with engineered enzymes. Future directions include increasing the H_2O_2 output of PdAu NPs under alkaline conditions, optimizing cofactor stability, and modifying the protein scaffold to further improve reactivity and selectivity. The application of this concept to other oxidations, as well as to asymmetric variants, may offer novel solutions for sustainable and selective C–H bond functionalization.

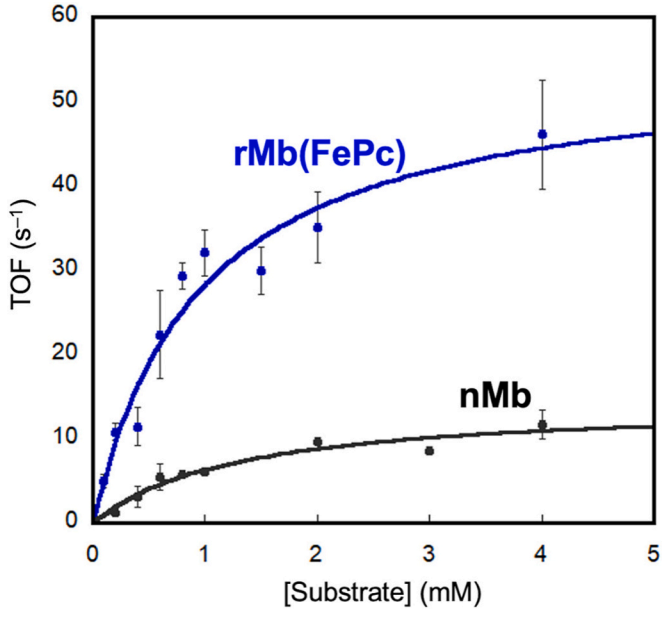

Fig. 4. Plots of TOF of catalytic C–H bond amination of 2,4,6-triisopropylbenzenesulfonyl azide. The plots were fitted by Michaelis Menten equations.

5. Rational design of an artificial ethylbenzene hydroxylase using molecular dynamics simulation

Hemeproteins have long served as promising scaffolds for catalyzing a broad range of natural and non-natural reactions. While nMb displays minimal catalytic activity relative to cytochrome P450, recent efforts combining genetic mutations and chemical modifications have unlocked Mb's potential as a versatile catalyst. However, achieving enantioselective C–H bond hydroxylation remains a major challenge, particularly for small, unfunctionalized substrates like ethylbenzene. In this context, a rational design strategy based on molecular dynamics (MD) simulations was employed to enhance the enantioselectivity of rMb(MnPc) for ethylbenzene hydroxylation. Initial experiments showed that wild-type

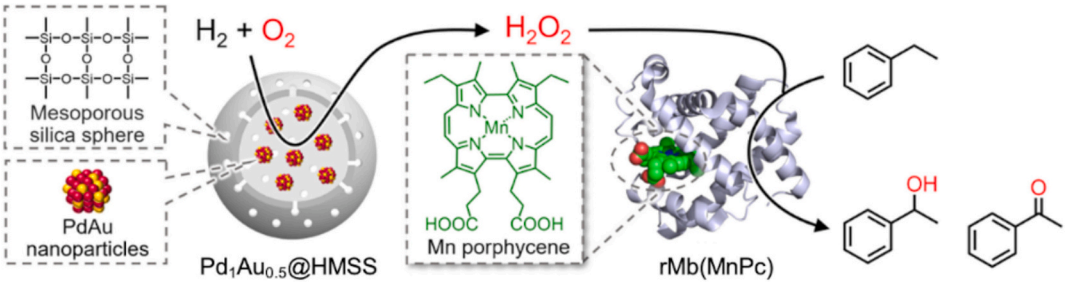

Fig. 5. Schematic representation of the hybrid catalysis by rMb(MnPc) and $Pd_1Au_{0.5}$@HMSS.

rMb(MnPc) catalyzed ethylbenzene hydroxylation with a modest 17 % ee favoring (*S*)-1-phenylethanol, while the H64A mutant improved ee to 43 % favoring the (*R*)-enantiomer. Recognizing the critical role of the distal His64 residue, we adopted a computational approach to predict promising mutations. Instead of quantum mechanical simulations, which are computationally intensive, MD simulations with angle constraints were utilized to model the active Mn(V)-oxo intermediate and substrate binding conformations. By constraining the Mn–O–H and O–H–C angles to 115° and 175° respectively—based on mechanistic insights from cytochrome P450—the productive *pro-S* and *pro-R* orientations were modeled (Fig. 6). Energy differences between the *pro-S* and *pro-R* binding conformations were calculated for a series of mutations at key residues (positions 29, 33, 43, 46, 64, 67, and 68). Favorable energy differentials indicated mutations likely to enhance selectivity toward one enantiomer. The MD-predicted values for wild-type rMb(MnPc) and the H64A mutant aligned with experimental observations, validating the use of this method for rational design. Subsequent experimental validation of selected mutants revealed striking improvements. Among single mutants, the F43A mutant provided the highest enantioselectivity for (*S*)-1-phenylethanol (56 % ee). At the same time, mutations at H64 (such as H64I and H64A) modulated enantioselectivity toward either (*S*)- or (*R*)-configuration, demonstrating that subtle alterations at the distal site significantly influence substrate positioning and reactive intermediate stabilization. Building on single mutation data, double and triple mutants were constructed to further enhance enantioselectivity. Remarkably, the F43A/H64I and F43A/H64I/V68F mutants achieved 68 % and 69 % ee, respectively, favoring (*S*)-1-phenylethanol. In contrast, for (*R*)-selective hydroxylation, the F46L/H64A mutant reached 57 % ee. The improvements observed in these multiple mutants suggest an additive effect between mutations, where each alteration independently biases substrate binding or transition state stabilization toward a particular enantiomer. To evaluate the reliability of the MD simulation-based design, the predicted energy differentials were correlated with experimental ee values (Fig. 7). A moderate correlation coefficient of $r = 0.66$ was obtained, improving to $r = 0.79$ when data points with small energy differences ($\leq$1 kcal/mol) were excluded. This result indicates that MD simulations, even at this level of approximation, provide useful guidance for enantioselective catalyst design. Furthermore, X-ray crystallographic analysis of selected mutants, including F43A/H64I and F46L/H64A, confirmed that the mutations did not perturb the overall protein fold (Fig. 8). Instead, subtle structural adjustments near the active site created cavities that facilitated enantioselective substrate binding, as predicted by the MD models. In the F43A/H64I mutant, removal of the Phe43 side chain generated a pocket accommodating ethylbenzene's phenyl group in the *pro-S* orientation, consistent with enhanced (*S*)-selectivity. Catalytic turnover numbers (TONs) were also determined for all mutants. While TONs varied across mutants, no clear correlation was found between TON and enantioselectivity. This observation is rational, as enantioselectivity is determined by the differential stabilization of transition states, whereas TON reflects a combination of factors including substrate binding, catalyst stability, and reaction kinetics. Importantly, no significant overoxidation to ketone products (acetophenone) was observed under the reaction conditions, indicating that hydroxylation to alcohol remains the dominant pathway. This selectivity further highlights the utility of the MnPc-based artificial metalloenzyme system for controlled C–H bond activation. Thus, this investigation demonstrates a successful rational design of an artificial ethylbenzene hydroxylase with improved enantioselectivity using MD simulations to predict productive substrate binding orientations. The approach provides a generalizable framework for the design of artificial metalloenzymes targeting challenging C–H functionalization reactions.

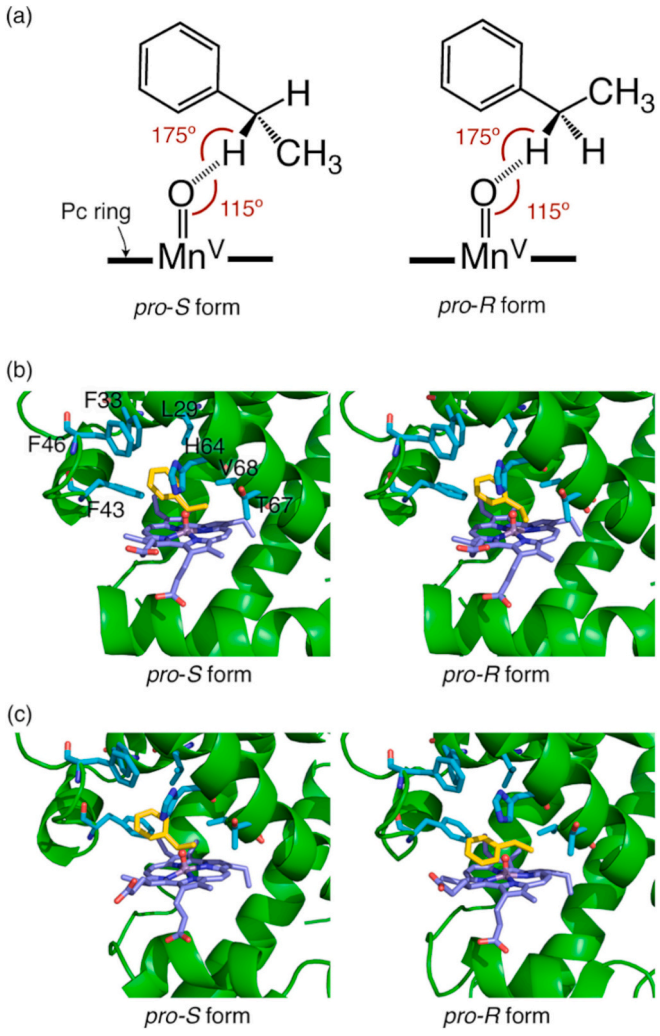

Fig. 6. (a) Angle constraints in MD simulations for *pro-S* and *pro-R* forms in the substrate binding. (b) Initial structures of active species of wild type rMb(MnPc) with ethylbenzene in *pro-S* and *pro-R* forms for the simulations. (c) Representative MD structures of the *pro-S* and *pro-R* forms after 5.0 ns simulations.

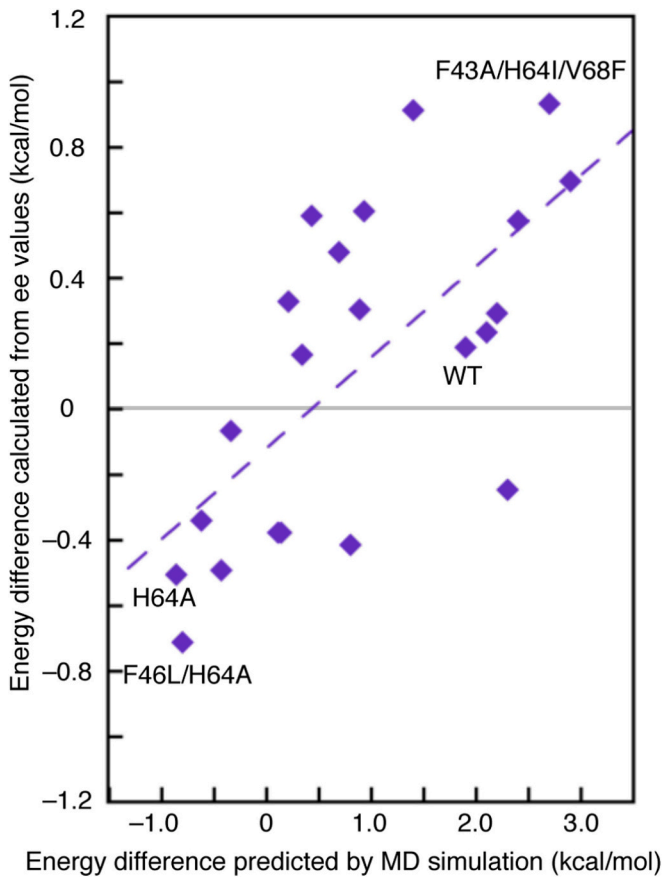

Fig. 7. Plots of experimentally determined energy difference from ee values in ethylbenzene hydroxylation against energy difference predicted by simulations for ethylbenzene binding for the rMb mutants.

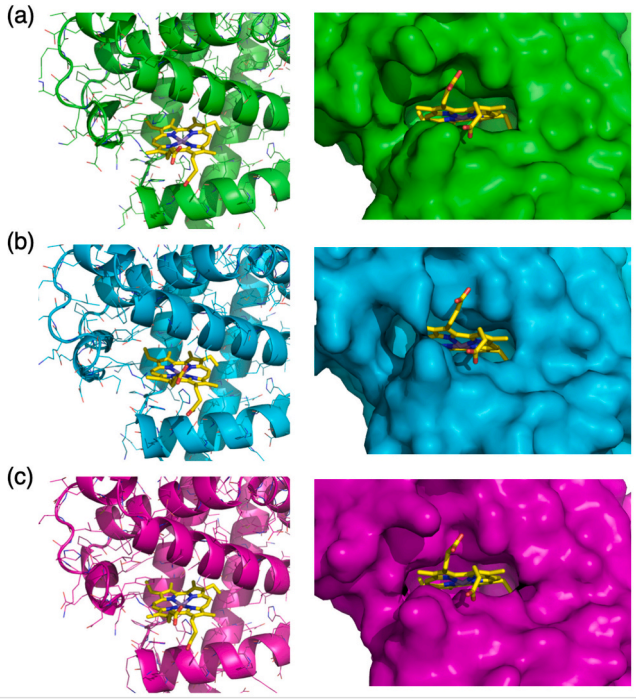

Fig. 8. Crystal structures of (a) wild type rMb(MnPc) (PDB ID: 8KFH), (b) the F43A/H64I mutant (PDB ID: 8KFI) and (c) the F46L/H64A mutant (PDB ID: 8KFJ).

Future efforts could expand this strategy to a wider range of substrates and active site modifications, paving the way toward practical and selective biocatalytic C–H activation.

6. Conclusion

Recent advances in engineering hemoproteins with non-canonical cofactors have significantly expanded the repertoire of artificial metalloenzymes. By integrating synthetic metal complexes into protein matrices and rationally designing surrounding environments through non-canonical amino acids and directed evolution, unique catalytic functions have been achieved that go beyond the scope of natural enzymes. Our studies demonstrate that the hydrophobic heme-binding pocket, in combination with tailored axial ligands, provides an ideal scaffold to regulate reactivity, modulate redox properties, and stabilize reactive intermediates such as metal-carbenes and metal-nitrenes. The successful observation and mechanistic analysis of reactive species within these engineered systems offer valuable insights for further catalyst development. Such control over intermediate lifetimes and transition states enables the rational design of catalysts for challenging transformations, including enantioselective C–H bond functionalization and aerobic oxidations. Hybrid catalysis approaches, combining protein-based catalysts with inorganic nanoparticles, further highlight the potential for artificial systems to emulate and surpass complex natural processes. In future, the precision engineering of both cofactors and protein environments promises to unlock “dream reactions” characterized by unparalleled levels of stereoselectivity, regioselectivity, and chemoselectivity. Continued interdisciplinary efforts at the interface of synthetic chemistry, protein engineering, and computational modeling will be essential for realizing the full potential of artificial metalloenzymes in sustainable synthesis and beyond.

CRediT authorship contribution statement

Koji Oohora: Writing – original draft, Conceptualization.

Declaration of competing interest

The authors declare that they have no known competing financial interests or personal relationships that could have appeared to influence the work reported in this paper.

Acknowledgements

KO thanks for his coworkers including graduate students who contributed to the results presented in this article as well as our collaborators named in the references cited. This work was supported by Grants-in-Aid for Scientific Research provided by JSPS KAKENHI Grant Numbers JP20KK0315, JP23H03832, JP24H01079, JP24H01855 and JP 25K01787 as well as JST PRESTO (JPMJPR22A3).

Data availability

Data will be made available on request.

References

[1] S.M. Cohen, A bioinorganic approach to fragment-based drug discovery targeting metalloenzymes, Acc. Chem. Res. 50 (2017) 2007–2016, https://doi.org/10.1021/acs.accounts.7b00242.
[2] R.H. Holm, P. Kennepohl, E.I. Solomon, Structural and functional aspects of metal sites in biology, Chem. Rev. 96 (1996) 2239–2314, https://doi.org/10.1021/cr9500390.
[3] M. Zhao, H.-B. Wang, L.-N. Ji, Z.-W. Mao, Insights into metalloenzyme microenvironments: biomimetic metal complexes with a functional second coordination sphere, Chem. Soc. Rev. 42 (2013) 8360, https://doi.org/10.1039/c3cs60162e.

[4] T.L. Poulos, Heme enzyme structure and function, Chem. Rev. 114 (2014) 3919–3962, https://doi.org/10.1021/cr400415k.
[5] S.P. De Visser, Second-coordination sphere effects on selectivity and specificity of heme and nonheme iron enzymes, Chem. A Eur. J. 26 (2020) 5308–5327, https://doi.org/10.1002/chem.201905119.
[6] B.A. Springer, S.G. Sligar, J.S. Olson, G.N. Jr Phillips, Mechanisms of ligand recognition in myoglobin, Chem. Rev. 94 (1994) 699–714, https://doi.org/10.1021/cr00027a007.
[7] Y. Yang, F.H. Arnold, Navigating the unnatural reaction space: directed evolution of heme proteins for selective carbene and nitrene transfer, Acc. Chem. Res. 54 (2021) 1209–1225, https://doi.org/10.1021/acs.accounts.0c00591.
[8] P.S. Coelho, E.M. Brustad, A. Kannan, F.H. Arnold, Olefin cyclopropanation via carbene transfer catalyzed by engineered cytochrome P450 enzymes, Science 339 (2013) 307–310, https://doi.org/10.1126/science.1231434.
[9] P.S. Coelho, Z.J. Wang, M.E. Ener, S.A. Baril, A. Kannan, F.H. Arnold, E.M. Brustad, A serine-substituted P450 catalyzes highly efficient carbene transfer to olefins in vivo, Nat. Chem. Biol. 9 (2013) 485–487, https://doi.org/10.1038/nchembio.1278.
[10] O.F. Brandenberg, C.K. Prier, K. Chen, A.M. Knight, Z. Wu, F.H. Arnold, Stereoselective enzymatic synthesis of heteroatom-substituted cyclopropanes, ACS Catal. 8 (2018) 2629–2634, https://doi.org/10.1021/acscatal.7b04423.
[11] A.M. Knight, S.B.J. Kan, R.D. Lewis, O.F. Brandenberg, K. Chen, F.H. Arnold, Diverse engineered heme proteins enable stereodivergent cyclopropanation of unactivated alkenes, ACS Cent. Sci. 4 (2018) 372–377, https://doi.org/10.1021/acscentsci.7b00548.
[12] Y. Wei, A. Tinoco, V. Steck, R. Fasan, Y. Zhang, Cyclopropanations via heme carbenes: basic mechanism and effects of carbene substituent, protein axial ligand, and porphyrin substitution, J. Am. Chem. Soc. 140 (2018) 1649–1662, https://doi.org/10.1021/jacs.7b09171.
[13] M. Bordeaux, V. Tyagi, R. Fasan, Highly diastereoselective and enantioselective olefin cyclopropanation using engineered myoglobin-based catalysts, Angew. Chem. Int. Ed. 54 (2015) 1744–1748, https://doi.org/10.1002/anie.201409928.
[14] D.A. Vargas, R.L. Khade, Y. Zhang, R. Fasan, Biocatalytic strategy for highly diastereo- and enantioselective synthesis of 2,3-dihydrobenzofuran-based tricyclic scaffolds, Angew. Chem. Int. Ed. 58 (2019) 10148–10152, https://doi.org/10.1002/anie.201903455.
[15] X. Zhang, D. Chen, J. Stropp, R. Tachibana, Z. Zou, D. Klose, T.R. Ward, Repurposing myoglobin into an abiological asymmetric ketoreductase, Chem 10 (2024) 2577–2589, https://doi.org/10.1016/j.chempr.2024.06.010.
[16] T.B. Silva, M. Spulber, M.K. Kocik, F. Seidi, H. Charan, M. Rother, S.J. Sigg, K. Renggli, G. Kali, N. Bruns, Hemoglobin and red blood cells catalyze atom transfer radical polymerization, Biomacromolecules 14 (2013) 2703–2712, https://doi.org/10.1021/bm400556x.
[17] Q. Zhou, M. Chin, Y. Fu, P. Liu, Y. Yang, Stereodivergent atom-transfer radical cyclization by engineered cytochromes P450, Science 374 (2021) 1612–1616, https://doi.org/10.1126/science.abk1603.
[18] W. Fu, N.M. Neris, Y. Fu, Y. Zhao, B. Krohn-Hansen, P. Liu, Y. Yang, Enzyme-controlled stereoselective radical cyclization to arenes enabled by metalloredox biocatalysis, Nat. Catal. 6 (2023) 628–636, https://doi.org/10.1038/s41929-023-00986-5.
[19] A. Lubskyy, C. Guo, R.J. Chadwick, A. Petri-Fink, N. Bruns, M.M. Pellizzoni, Engineered myoglobin as a catalyst for atom transfer radical cyclisation, Chem. Commun. 58 (2022) 10989–10992, https://doi.org/10.1039/D2CC03227A.
[20] N.Y. Shin, J.M. Ryss, X. Zhang, S.J. Miller, R.R. Knowles, Light - driven deracemization enabled by excited-state electron transfer, Science 366 (2019) 364–369, https://doi.org/10.1126/science.aay2204.
[21] B. Brouwer, F. Della-Felice, J.H. Illies, E. Iglesias-Moncayo, G. Roelfes, I. Drienovská, Noncanonical amino acids: bringing new-to-nature functionalities to biocatalysis, Chem. Rev. 124 (2024) 10877–10923, https://doi.org/10.1021/acs.chemrev.4c00136.
[22] K. Oohora, A. Onoda, T. Hayashi, Hemoproteins reconstituted with artificial metal complexes as biohybrid catalysts, Acc. Chem. Res. 52 (2019) 945–954, https://doi.org/10.1021/acs.accounts.8b00676.
[23] K. Oohora, T. Hayashi, Myoglobins engineered with artificial cofactors serve as artificial metalloenzymes and models of natural enzymes, Dalton Trans. 50 (2021) 1940–1949, https://doi.org/10.1039/D0DT03597A.
[24] M. Pott, T. Hayashi, T. Mori, P.R.E. Mittl, A.P. Green, D. Hilvert, A noncanonical proximal heme ligand affords an efficient peroxidase in a globin fold, J. Am. Chem. Soc. 140 (2018) 1535–1543, https://doi.org/10.1021/jacs.7b12621.
[25] T. Hayashi, M. Tinzl, T. Mori, U. Krengel, J. Proppe, J. Soetbeer, D. Klose, G. Jeschke, M. Reiher, D. Hilvert, Capture and characterization of a reactive haem–carbenoid complex in an artificial metalloenzyme, Nat. Catal. 1 (2018) 578–584, https://doi.org/10.1038/s41929-018-0105-6.
[26] M. Pott, M. Tinzl, T. Hayashi, Y. Ota, D. Dunkelmann, P.R.E. Mittl, D. Hilvert, Noncanonical heme ligands steer carbene transfer reactivity in an artificial metalloenzyme**, Angew. Chem. Int. Ed. 60 (2021) 15063–15068, https://doi.org/10.1002/anie.202103437.
[27] E.L. Onderko, A. Silakov, T.H. Yosca, M.T. Green, Characterization of a selenocysteine-ligated P450 compound I reveals direct link between electron donation and reactivity, Nat. Chem. 9 (2017) 623–628, https://doi.org/10.1038/nchem.2781.
[28] X. Liu, Y. Yu, C. Hu, W. Zhang, Y. Lu, J. Wang, Significant increase of oxidase activity through the genetic incorporation of a tyrosine–histidine cross-link in a myoglobin model of heme–copper oxidase, Angew. Chem. Int. Ed. 51 (2012) 4312–4316, https://doi.org/10.1002/anie.201108756.
[29] H.M. Key, P. Dydio, D.S. Clark, J.F. Hartwig, Abiological catalysis by artificial haem proteins containing noble metals in place of iron, Nature 534 (2016) 534–537, https://doi.org/10.1038/nature17968.
[30] P. Dydio, H.M. Key, A. Nazarenko, J.Y.-E. Rha, V. Seyedkazemi, D.S. Clark, J. F. Hartwig, An artificial metalloenzyme with the kinetics of native enzymes, Science 354 (2016) 102–106, https://doi.org/10.1126/science.aah4427.
[31] Y. Gu, S.N. Natoli, Z. Liu, D.S. Clark, J.F. Hartwig, Site-selective functionalization of (sp^3)C–H bonds catalyzed by artificial metalloenzymes containing an iridium-porphyrin cofactor, Angew. Chem. Int. Ed. 58 (2019) 13954–13960, https://doi.org/10.1002/anie.201907460.
[32] H.M. Key, P. Dydio, Z. Liu, J.Y.-E. Rha, A. Nazarenko, V. Seyedkazemi, D.S. Clark, J.F. Hartwig, Beyond iron: iridium-containing P450 enzymes for selective cyclopropanations of structurally diverse alkenes, ACS Cent. Sci. 3 (2017) 302–308, https://doi.org/10.1021/acscentsci.6b00391.
[33] P. Dydio, H.M. Key, H. Hayashi, D.S. Clark, J.F. Hartwig, Chemoselective, enzymatic C–H bond amination catalyzed by a cytochrome P450 containing an Ir (Me)-PIX cofactor, J. Am. Chem. Soc. 139 (2017) 1750–1753, https://doi.org/10.1021/jacs.6b11410.
[34] M.W. Wolf, D.A. Vargas, N. Lehnert, Engineering of RuMb: toward a Green catalyst for Carbene insertion reactions, Inorg. Chem. 56 (2017) 5623–5635, https://doi.org/10.1021/acs.inorgchem.6b03148.
[35] G. Sreenilayam, E.J. Moore, V. Steck, R. Fasan, Metal substitution modulates the reactivity and extends the reaction scope of myoglobin carbene transfer catalysts, Adv. Synth. Catal. 359 (2017) 2076–2089, https://doi.org/10.1002/adsc.201700202.
[36] R. Alcala-Torano, N. Halloran, N. Gwerder, D.J. Sommer, G. Ghirlanda, Light-driven CO_2 reduction by Co-cytochrome b_{562}, Front. Mol. Biosci. 8 (2021) 609654, https://doi.org/10.3389/fmolb.2021.609654.
[37] Y. Deng, S. Dwaraknath, W.O. Ouyang, C.J. Matsumoto, S. Ouchida, Y. Lu, Engineering an oxygen-binding protein for photocatalytic CO_2 reductions in water, Angew. Chem. Int. Ed. 62 (2023) e202215719, https://doi.org/10.1002/anie.202215719.
[38] Y.-B. Cai, X.-H. Li, J. Jing, J.-L. Zhang, Effect of distal histidines on hydrogen peroxide activation by manganese reconstituted myoglobin, Metallomics 5 (2013) 828, https://doi.org/10.1039/c3mt20275e.
[39] R.J. Labidi, B. Faivre, P. Carpentier, J. Perard, P. Gotico, Y. Li, M. Atta, M. Fontecave, Light-activated artificial CO_2 -reductase: structure and activity, J. Am. Chem. Soc. (2024) 28296–28305, https://doi.org/10.1021/jacs.4c08927.
[40] T. Matsuo, D. Murata, Y. Hisaeda, H. Hori, T. Hayashi, Porphyrinoid chemistry in hemoprotein matrix: detection and reactivities of iron(IV)-oxo species of porphycene incorporated into horseradish peroxidase, J. Am. Chem. Soc. 129 (2007) 12906–12907, https://doi.org/10.1021/ja074685f.
[41] K. Oohora, H. Meichin, L. Zhao, M.W. Wolf, A. Nakayama, J. Hasegawa, N. Lehnert, T. Hayashi, Catalytic cyclopropanation by myoglobin reconstituted with iron porphycene: acceleration of catalysis due to rapid formation of the carbene species, J. Am. Chem. Soc. 139 (2017) 17265–17268, https://doi.org/10.1021/jacs.7b10154.
[42] K. Oohora, Y. Miyazaki, T. Hayashi, Myoglobin reconstituted with Ni tetradehydrocorrin as a methane-generating model of methyl-coenzyme M reductase, Angew. Chem. Int. Ed. 58 (2019) 13813–13817, https://doi.org/10.1002/anie.201907584.
[43] Y. Miyazaki, K. Oohora, T. Hayashi, Focusing on a nickel hydrocorphinoid in a protein matrix: methane generation by methyl-coenzyme M reductase with F430 cofactor and its models, Chem. Soc. Rev. 51 (2022) 1629–1639, https://doi.org/10.1039/D1CS00840D.
[44] Y. Morita, K. Oohora, E. Mizohata, A. Sawada, T. Kamachi, K. Yoshizawa, T. Inoue, T. Hayashi, Crystal structures and coordination behavior of aqua- and Cyano-Co (III) tetradehydrocorrins in the heme pocket of myoglobin, Inorg. Chem. 55 (2016) 1287–1295, https://doi.org/10.1021/acs.inorgchem.5b02598.
[45] Y. Miyazaki, K. Oohora, T. Hayashi, Methane generation and reductive debromination of benzylic position by reconstituted myoglobin containing nickel tetradehydrocorrin as a model of methyl-coenzyme M reductase, Inorg. Chem. 59 (2020) 11995–12004, https://doi.org/10.1021/acs.inorgchem.0c00901.
[46] D.M. Carminati, R. Fasan, Stereoselective cyclopropanation of electron-deficient olefins with a cofactor redesigned carbene transferase featuring radical reactivity, ACS Catal. 9 (2019) 9683–9697, https://doi.org/10.1021/acscatal.9b02272.
[47] Y. Kagawa, K. Oohora, T. Himiyama, A. Suzuki, T. Hayashi, Redox engineering of myoglobin by cofactor substitution to enhance cyclopropanation reactivity, Angew. Chem. Int. Ed. 63 (2024) e202403485, https://doi.org/10.1002/anie.202403485.
[48] Y. Kagawa, K. Oohora, T. Hayashi, Intramolecular C-H bond amination catalyzed by myoglobin reconstituted with iron porphycene, J. Inorg. Biochem. 252 (2024) 112459, https://doi.org/10.1016/j.jinorgbio.2023.112459.
[49] K. Oohora, Y. Kagawa, Y. Kuwahara, H. Yamashita, T. Hayashi, Ethylbenzene oxidation by a hybrid catalysis system of reconstituted myoglobin and silica-protected PdAu nanoparticles under a hydrogen-oxygen mixed atmosphere, J. Porphyrins Phthalocyanines 27 (2023) 1313–1319, https://doi.org/10.1142/S1088424623500906.
[50] K. Oohora, Y. Kagawa, T. Nishiura, E. Mizohata, U. Schwaneberg, T. Hayashi, Rational design of an artificial ethylbenzene hydroxylase using a molecular dynamics simulation to enhance enantioselectivity, Chem. Lett. 53 (2024) upad042, https://doi.org/10.1093/chemle/upad042.

[51] K. Oohora, Y. Kihira, E. Mizohata, T. Inoue, T. Hayashi, C(sp^3)–H bond hydroxylation catalyzed by myoglobin reconstituted with manganese porphycene, J. Am. Chem. Soc. 135 (2013) 17282–17285, https://doi.org/10.1021/ja409404k.
[52] K. Oohora, H. Meichin, Y. Kihira, H. Sugimoto, Y. Shiro, T. Hayashi, Manganese(V) porphycene complex responsible for inert C–H bond hydroxylation in a myoglobin matrix, J. Am. Chem. Soc. 139 (2017) 18460–18463, https://doi.org/10.1021/jacs.7b11288.
[53] S. Masuda, K. Mori, Y. Kuwahara, H. Yamashita, PdAg nanoparticles supported on resorcinol-formaldehyde polymers containing amine groups: the promotional effect of phenylamine moieties on CO_2 transformation to formic acid, J Mater Chem A 7 (2019) 16356–16363, https://doi.org/10.1039/C9TA02552A.